Research Article

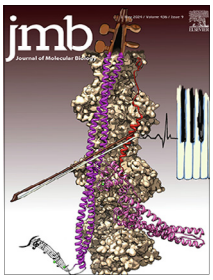

Proline Peptide Bond Isomerization in Ubiquitin Under Folding and Denaturing Conditions by Pressure-Jump NMR

Elahe Masoumzadeh, Jinfa Ying, James L. Baber, Philip Anfinrud and Ad Bax *

Laboratory of Chemical Physics, *National Institute of Diabetes and Digestive and Kidney Diseases, National Institutes of Health, Bethesda, MD 20892, USA*

Correspondence to Ad Bax: *bax@nih.gov (A. Bax)*
https://doi.org/10.1016/j.jmb.2024.168587
Edited by C. Kalodimos

Abstract

Proline isomerization is widely recognized as a kinetic bottleneck in protein folding, amplified for proteins rich in Pro residues. We introduced repeated hydrostatic pressure jumps between native and pressure-denaturing conditions inside an NMR sample cell to study proline isomerization in the pressure-sensitized L50A ubiquitin mutant. Whereas in two unfolded heptapeptides, X-Pro peptide bonds isomerized *ca* 1.6-fold faster at 1 bar than at 2.5 kbar, for ubiquitin *ca* eight-fold faster isomerization was observed for Pro-38 and *ca* two-fold for Pro-19 and Pro-37 relative to rates measured in the pressure-denatured state. Activation energies for isomerization in pressure-denatured ubiquitin were close to literature values of 20 kcal/mole for denatured polypeptides but showed a substantial drop to 12.7 kcal/mole for Pro-38 at atmospheric pressure. For ubiquitin isomers with a *cis* E18-P19 peptide bond, the 1-bar NMR spectrum showed sharp resonances with near random coil chemical shifts for the C-terminal half of the protein, characteristic of an unfolded chain, while most of the N-terminal residues were invisible due to exchange broadening, pointing to a metastable partially folded state for this previously recognized 'folding nucleus'. For *cis*-P37 isomers, a drop in pressure resulted in the rapid loss of nearly all unfolded-state NMR resonances, while the recovery of native state intensity revealed a slow component attributed to *cis* → *trans* isomerization of P37. This result implies that the NMR-invisible *cis*-P37 isomer adopts a molten globule state that encompasses the entire length of the ubiquitin chain, suggestive of a structure that mostly resembles the folded state.

Published by Elsevier Ltd.

Introduction

One important aspect of protein folding concerns the role of proline *cis/trans* isomerization because the high energetic barrier associated with this process, *ca* 20 kcal/mole,[1] often strongly slows down the folding rate of isomers that contain non-native X-Pro peptide bonds. The presence of non-native proline isomers during protein folding can promote aggregation and has been implicated in amyloid formation.[2] However, proline isomerization can be greatly accelerated by peptidyl-prolyl cis/-trans isomerase enzymes, such as trigger factor which is part of the *E. coli* 50S ribosomal subunit.[3,4] A host of other widely studied isomerases, including cyclophilin,[5–7] FK506 binding protein (FKBP),[8] and Pin1,[9,10] are well recognized immunophilins, testifying to the biological importance of the isomerization process.

In a polypeptide, the steric clash between $C^{\alpha}H^{\alpha}$ groups of sequential non-Pro residues with an intervening *cis* peptide bond raises the energy over *trans* conformations by *ca* 3–4 kcal/mole. This energy difference is much smaller for Pro residues, *ca* 1–2 kcal/mole, because of a steric clash between the Pro $C^{\delta}H^{\delta}$ moiety and the $C^{\alpha}H^{\alpha}$

of its preceding residue in the *trans* isomer.[1] In the unfolded state near room temperature, the equilibrium population of X-Pro *cis* peptide bonds covers a broad range from $\leq$3% to $\geq$30%.[11–13] This fraction depends on the residue types neighboring the Pro, with highest values found when the residue preceding or following Pro is aromatic.[12] The *cis* fractions are a few percent higher for X-Pro bonds in short linear peptides compared to longer disordered polypeptide chains,[13] presumably due to increased steric clashes between the chains N-terminal and C-terminal to a *cis* X-Pro peptide bond which raises their free energy.[11]

Any given X-Pro peptide bond in a natively folded protein typically is either 100% *trans* or, less often, 100% *cis*. In rare but important cases, proline *cis*/*trans* isomerization can serve as a slow functional switch, altering the protein's structure and its ability to bind ligands or interact with other biomolecules.[14–16] Pro isomerization has been studied most extensively by fluorescence-based methods that provide information on the environment of a fluorophore, most commonly tryptophan, which depends on its solvent exposure. Such fluorescence measurements report on the global structure of the protein which depends upon the *cis/trans* equilibrium of its Pro residues. Assigning the observed effects to individual Pro residues often relies on site-directed mutagenesis but is difficult to probe in structural detail because of small fractions of non-native *cis* isomers. By contrast, NMR spectroscopy provides residue-specific information on the effect of *cis* and *trans* prolyl bonds throughout the entire protein. NMR experiments which include jumps in the hydrostatic pressure that are repeated thousands of times,[17,18] then permit the monitoring of the relation between specific prolyl isomeric states and protein structure, even in very large oligomeric aggregates.[19]

Here, we used pressure-jump NMR to evaluate the effect of non-native prolyl peptide bonds on the structure and folding of ubiquitin, a widely studied model system containing three proline residues. Single and double pressure jump experiments were used to monitor the isomerization kinetics under both folding and unfolding conditions, covering a wide range of time scales. Because human ubiquitin is an exceptionally stable protein, requiring over 5 kbar of pressure to unfold,[20] we introduced a cavity into the protein structure by the L50A mutation. Such a mutation sensitizes the protein to hydrostatic pressure,[21,22] yielding an unfolding mid-point for L50A ubiquitin of *ca* 1.2 kbar at 278 K, well within reach of our pressure-jump instrumentation.

We found that L50A ubiquitin can partially fold before each X-Pro bond has isomerized to its final state. Moreover, the changed energy landscape in such a partially folded protein containing the non-native peptidyl isomer can result in faster isomerization than observed in the unfolded state.

Materials and Methods

Protein expression and purification. Perdeuterated protein was used for all measurements because it yields superior spectral resolution and sensitivity. A plasmid encoding the sequence of the L50A mutant of human ubiquitin was obtained from Genscript and transformed into *E. coli* BL21(DE3) competent cells. Following overnight growth at 37 °C in 5 mL Luria-Bertani (LB) culture medium, the cells were spun down and transferred to 50 mL of M9 minimal medium containing 1 g/L of $^{15}NH_4Cl$ in 99.8% D_2O. This culture was grown at 37 °C for 3 h, and then the cells were transferred into 0.5 L of the same M9 minimal medium in D_2O. When the optical density reached *ca* 0.7, protein expression was initiated by addition of 1 mM IPTG and allowed to proceed for 4 h at 37 °C. The cells were then harvested and stored at −80 °C. Cell pellets were resuspended in 50 mM Tris-HCl buffer, pH 7.6, and lysed using a Cell Disruptor (Constant Systems Ltd), with multiple passages of the cells at 2.2 kbar. The lysed cells were spun at 50,000 g for 20 min at 4 °C, after which the supernatant was collected, and the pH adjusted to 3.3 using acetic acid to precipitate contaminants. The pH 3.3 sample was spun at 50,000 g for 20 min at 4 °C, and the supernatant was loaded onto a Superdex S75 26/60 column (GE Healthcare) that was equilibrated with 10 mM potassium buffer at pH 6.8. The ubiquitin-containing fractions were collected, concentrated, and then subjected to reverse-phase HPLC using a Vydac 214TP C4 column. The HPLC purification step is essential for high-pressure NMR measurements because at high pressure the unfolded protein is highly susceptible to proteolysis by residual trace amounts of protease. Ubiquitin L50A eluted around 38% acetonitrile containing 0.1% trifluoroacetic acid and was subsequently lyophilized. Lyophilized protein was dissolved in 20 mM phosphate buffer, pH 6.4, containing 1 mM EDTA and 1 mM benzamidine as broad-spectrum protease inhibitors, and 3% D_2O for NMR field-frequency lock purposes.

NMR spectroscopy. Spectra were recorded on Bruker NEO spectrometers operating at 600, 800, and 900 MHz, each equipped with a cryogenically cooled probehead and a home-built pressure-jump accessory.[18] Typically, 220 μL of 0.4 mM ^{15}N-Ubiquitin L50A solution was loaded into a high-pressure tube (Daedalus Innovations, Aston, PA), and pressurized up to 2.4 kbar for measurements. The pressure-jump accessory uses mineral spirits as a low-viscosity hydraulic fluid with a density lower than water. It enables rapid switching of the hydrostatic pressure inside the NMR sample cell between atmospheric pressure and pressures up to 3 kbar, limited by the strength of the NMR sample cell. The time needed for switching the pressure is

also adjustable and was increased to a few milliseconds to minimize cavitation at the aqueous/mineral spirits interface during depressurization, which can, after a large number of pressure cycles, lead to sample emulsification and contamination.

3D HNCO and HNCA spectra were recorded for resonance assignment of the folded protein (BMRB id: 52343) as well as those of the *trans* isomers (BMRB id: 52344) and the lowly populated *cis*-Pro isomers in the pressure-denatured state. Reconstruction of the non-uniformly sampled (NUS) 3D spectra was carried out using the SMILE program.[23] All spectra were processed using NMRPipe software[24] and analyzed with CCPN software.[25]

Equilibrium populations of *cis* isomers under denaturing conditions (2.4 kbar) were established from the relative integrated intensity of ^{1}H-^{15}N correlations in HSQC spectra[26] for resonances neighboring each of the three Pro residues. These spectra were recorded with a long delay (5 s) between scans, such as to minimize the effect of any small differences in ^{1}H T_1 between unfolded *cis* and *trans* isomers. For monitoring the rate of change in *cis* and *trans* isomer populations following a jump in pressure, 2D SOFAST-HMQC spectra typically were recorded with 70–90 complex t_1 increments and two scans per free induction decay (FID), with the measurement preceded by 16 "dummy scans" to establish a steady-state level of magnetization. For SOFAST-HMQC measurements at low pressure, signals were recorded at a rate of 2 scans s^{-1}, for a total measurement time of *ca* three minutes per 2D spectrum. For the double-jump measurements (Figure 4a), where the data are recorded at high pressure, signals were recorded at a rate of 4.3 s^{-1} (1 min per 2D spectrum; 70 complex t_1 increments) to minimize the effect of isomerization after the return to high pressure (see SI Text). The measurements (including pressure jumps) were repeated multiple times with separately recorded spectra co-added for improving signal to noise, prior to analysis.

Temperature equilibration. The very slow isomerization of the I36-P37 peptide bond, in particular at temperatures below 288 K, greatly lengthens the time needed to approach the equilibrium *cis*-P37 population in the unfolded state. To reduce this equilibration time, a stepwise temperature change protocol was used. First, the sample was pressurized to 2.4 kbar and kept at 298 K for 0.5 hr, after which the fraction of *cis* P37, averaged over the folded and unfolded species, was found to be 3.5%. One hour after dropping the temperature to 288 K, it grew further to 4.7%, and after an additional 2 h at 276 K it reached 5.2%, approaching its equilibrium value. In contrast, *cis*–*trans* equilibration in the pressure-denatured state for P38 is nearly an order of magnitude faster, permitting correspondingly shorter equilibration times at high pressure, faster repetition of the measurement, and improved S/N by averaging repeated measurements. The equilibrium fraction of *cis* P38 was found to be only 2.6%, requiring the averaging of four measurements for final data analysis.

Results

There are three Pro residues (P19, P37, and P38) in the Ubiquitin sequnce. Typically, in the unfolded state ^{1}H-^{15}N HSQC spectrum, *cis*-Pro isomer signals are resolved from *trans* signals for neighboring residues, up to $i \pm 3$ relative to the Pro residue in position *i*.{Alderson, 2018 #6512} Resonance assignments of both the pressure-denatured and native states of L50A ubiquitin were derived from standard 3D HNCO and HNCA spectra. With the exception of the mutation site, chemical shifts in the native state closely follow those of wild-type (WT) ubiquitin (Figure S1),[27] indicating that the 3D structure of the L50A mutant is essentially the same as that of WT. Similarly, with the exception of mutated residues, in the unfolded state the amide chemical shifts are very close to those of the previously studied V17A/V26A ubiquitin double mutant (Figure S2).[18] At low contour levels, resonances of the *cis* isomers are readily identified in the pressure-denatured HSQC spectrum (Figure S3) and these were used to monitor their populations, which were within experimental uncertainty of those reported previously[28] for the V17A/V26A ubiquitin double mutant (Table 1). For *cis*-P19, the best resolved HSQC signals in the unfolded state are observed for S20 and D21; for *cis*-P37, G35 and I36 are well resolved marker signals; for *cis*-P38, G35 and D39 are the characteristic markers (Figure S3). Upon dropping the pressure, unfolded chains with all-*trans* Pro residues rapidly fold back to their native state at a rate similar to that previously reported for the V17A/V26A double mutant ($k_{fold} \approx 1$ s^{-1};[18]).

Isomerization kinetics at high pressure

All three Pro residues in ubiquitin (P19, P37, and P38) are 100% *trans* in the equilibrated folded protein at atmospheric pressure. In the single-jump, high-pressure readout HSQC experiments, the unfolding process is initiated by a pressure-jump from 1 bar to 2.4 kbar, followed by a series of 10-minute ^{1}H-^{15}N HSQC measurements until the *cis*–*trans* equilibration is largely complete (Figure 1a). Upon the initial increase in pressure, the solvent temperature increases by *ca* 2 °C due to adiabatic compression of the solvent, after which the solution temperature cools to the temperature of the zirconium sample cell (Figure S4). After a 20-second temperature equilibration delay, a 40-second automated optimization of the magnetic field homogeneity precedes the start of the HSQC-series.

Table 1 Equilibrium *cis* populations (*cis*%^{HP}) and isomerization rates (hr^{-1}) at 2.4kbar (k_{ct}^{HP} and k_{ex}^{HP}) and 1 bar (k_{ct}^{AP}) at 276 K, and Arrhenius activation energies (kcal/mole) for three Pro residues in L50A ubiquitin at 2.4kbar (E_A^{HP}) and 1 bar (E_A^{AP}). AP and HP denote atmospheric pressure and high pressure (2.4 kbar), respectively.

	cis%^{HP}	k_{ct}^{HP}	k_{ex}^{HP}	k_{ct}^{AP}	E_A^{HP}	E_A^{AP}
P19	8.9 ± 0.4	1.49 ± 0.05	1.64 ± 0.06	3.26 ± 0.28	18.8 ± 0.5	16.3 ± 1.4
P37	6.2 ± 0.4	0.29 ± 0.01	0.31 ± 0.01	0.68 ± 0.17	20.6 ± 0.9	17.8 ± 1.8
P38	2.6 ± 0.4	2.7 ± 0.1	2.8 ± 0.2	23.4 ± 4.2	18.9 ± 1.1	12.7 ± 2.5

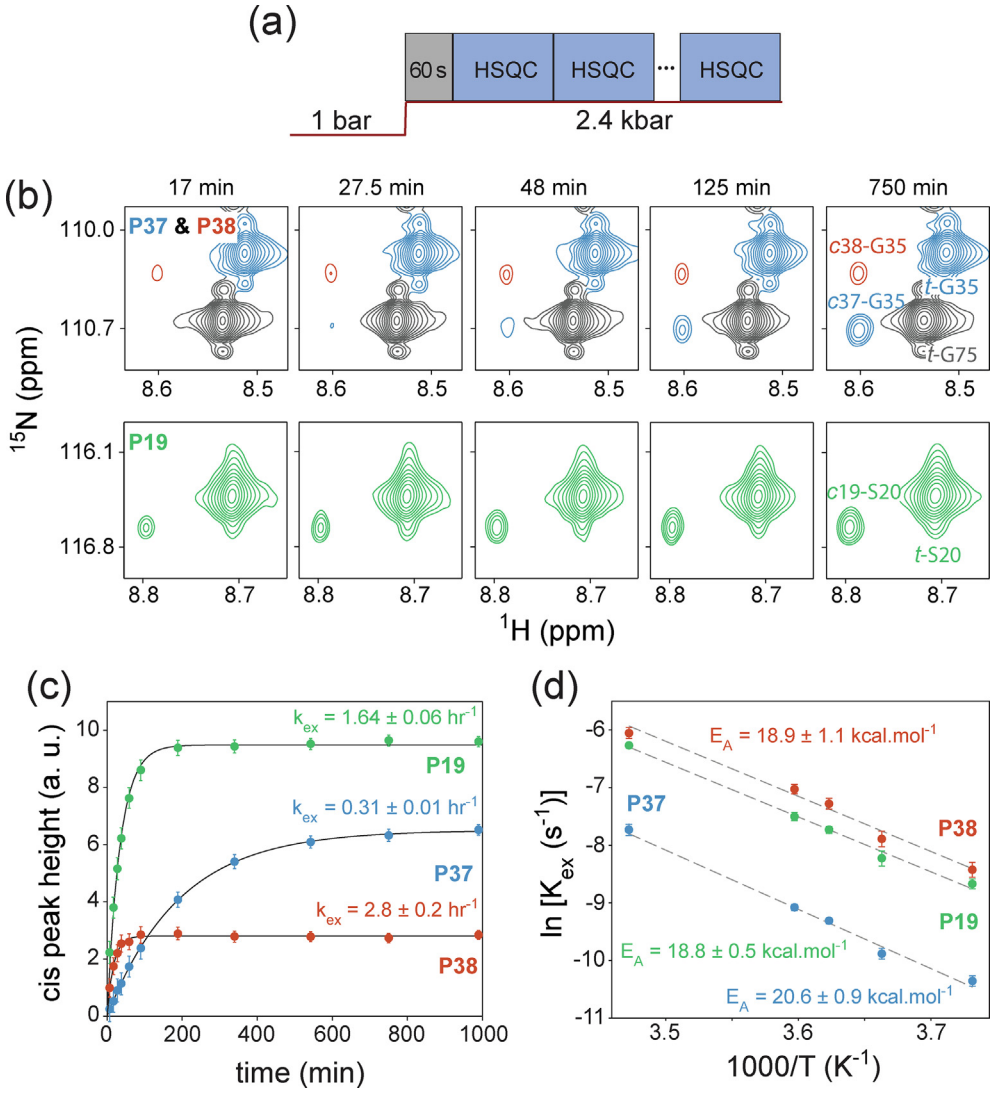

Figure 1. Pro isomerization kinetics at high pressure. (a) Schematic timing diagram for the single-jump, high-pressure readout HSQC experiments. After jumping the pressure to 2.4 kbar, a 20-s delay for temperature equilibration and a 40-s delay for shimming precede the recording of a series of HSQC spectra for a total duration of 12.5 h. (b) Expanded spectral regions showing (top row) G35(*cis*-P37, blue; *cis*-P38, red; *trans*-P37/P38, blue), and S20 (bottom row), recorded at 800 MHz, 276 K. "Wings" that symmetrically flank intense *trans* signals of G35 and G75 in the ^{15}N dimension result from truncation of the ^{15}N time domain data. (c) Growth of *cis* isomer populations for P19 (green), P37 (blue) and P38 (red). For other temperatures, see Figure S9. (d) Temperature dependence of k_{ex} for the three Pro residues and corresponding Arrhenius activation energies, E_A, related to the exchange rates by the Arrhenius equation $k_{ex} = A\ e^{-Ea/RT}$.

For P37 and P38, the *cis* fractions are most easily measured from the intensity of the well-resolved G35 amide resonances, which both shift downfield by *ca* 0.09 ppm in the ^{1}H dimension and by 0.6 and 0.2 ppm in ^{15}N for *cis*-P37 and *cis*-P38, respectively (Figure 1b). Similarly, the *cis*

population of P19 is derived from the well-resolved S20 amide correlations (Figure 1b). For measurements carried out at 276 K, P38 already approaches its equilibrium *cis* fraction within 0.5 h after pressurization, whereas P37 requires more than 3 h. As expected, populations of the unfolded *cis* fractions approach their Boltzmann equilibrium values as a mono-exponential function, from which the isomerization exchange rates, $k_{ex} = k_{ct} + k_{tc}$, are readily extracted (Figure 1c).

Repeats of the above measurements over the range from 268-288 K yielded the temperature dependence of the *cis–trans* exchange rates, from which the Arrhenius activation energies were derived (Figure 1d; Table 1). Observed values of 19 to 21 kcal/mol are in good agreement with literature values for *cis–trans* isomerization in unfolded polypeptides.[29,30] We note that the exchange rate is determined by the free energy barrier height, *i.e.* it includes the entropic term which factors out in the Arrhenius equation. Differences in k_{ex} for Pro residues with very similar Arrhenius activation energies therefore point to differences in the entropic contribution to the barrier.

Prior measurements of the hydrostatic pressure dependence of the proline isomerization rates in small peptide analogs showed a slow-down of k_{ex} with increasing pressure, corresponding to an activation volume, $\Delta V^{\ddagger} = 7.5 \pm 1$ cm^3/mol.[31] Here, we measured the Pro isomerization rates in two heptapeptides, acetyl-EVEPSDT-NH_2, mimicking the sequence surrounding P19 (9.6 ± 0.8% *cis*) and acetyl-EVFPSDT where the *cis* fraction was higher (18.9 ± 1.2%) due to the aromatic Phe residue preceding Pro.[32] Isomerization rates were measured at both atmospheric and 2.5 kbar pressures, using standard 2D exchange spectroscopy[33] at 327 K (Figure S5). A *ca* 1.6-fold slowdown in k_{ex} at 2.5 kbar over atmospheric pressure was observed for both peptides, corresponding to an activation volume $\Delta V^{\ddagger} \approx 5.4 \pm 1$ cm^3/mol for both peptides, somewhat smaller than previously observed for the much smaller N-acetyl-L-proline-NH-methylamide peptide mimetic.[31] Our lower $\Delta V^{\ddagger}$ follows predictions that N-substituents with larger mass decrease the barrier crossing speed, thereby providing more time for water molecules to rearrange during the peptide bond flip and thus reducing the formation of void space.[31]

Proline isomerization under folding conditions after pressure drop

Promptly after dropping the pressure from 2.4 kbar to 1 bar (Figure 2a), chains with all-*trans* Pro isomers rapidly fold to their native state, as observed by the recovery of the native state NMR resonance positions and line widths.[18] However, chains for which one of the three Pro residues is *cis* at the time of the pressure drop clearly cannot reach native state before isomerization to *trans* has occurred. Therefore, these chains initially have populations of *cis*-Pro isomers that were present in the pressure-denatured state, which then decrease at rates k_{ct} because at atmospheric pressure $k_{tc} \ll k_{fold}$ for proteins that have isomerized to *trans*, *i.e.* k_{tc} is effectively zero. The k_{ct} rate at atmospheric pressure cannot be slowed down by lowering the sample temperature to the same extent as was possible for k_{ex} measurements at high pressure, where the freezing point of water is strongly depressed. Moreover, the adiabatic expansion of the solvent upon jumping to low pressure temporarily cools the solvent by 2.3 K and we found that, in contrast to static samples, supercooling of the solution to below 273 K immediately after the pressure jump was not possible. Therefore, the lowest temperature accessible to pressure-jump experiments designed to determine k_{ct} at atmospheric pressure was 275 K. To keep a margin of safety, the actual lowest temperature setting used was 276 K. However, gradually lowering the temperature over a period of a few minutes following the drop in pressure permitted measurements down to 267.9 K (Figure S6). At this time, the population of chains containing *cis*-P38, the fastest isomerizing and lowest populated Pro in ubiquitin, was found to be below the detection threshold. Importantly, at 276 K, collection of a 3-minute SOFAST-HMQC spectrum that started 1 min after the pressure drop (Figure S8) also does not reveal the *cis*-P38 resonances for G35, I36, and D39, and also lacks the corresponding *cis*-P37 resonances, even though these were visible at 267.9 K (Figure S6). However, low-intensity resonances at near-random-coil positions remain visible after the pressure drop for most of the C-terminal half of the protein and for the *cis*-P19 position of residue S20 (green resonances in Figure 2b and Figures S6–S8). The rate of disappearance for the C-terminal resonances after the pressure drop matches that of the $S20_{P19cis}$ resonance (Figure 2c), thus assigning these weak resonances to *cis*-P19 chains. With few exceptions (G10, *K*11, T14, S20 and V26, and A28), no such resonances are observed for residues preceding G35 (Figure S7).

The few observed N-terminal resonances for *cis*-P19 chains are weak relative to those of the unfolded C-terminal half of the protein (Figure S7). These weak N-terminal residues also exhibit smaller ^{15}N chemical shift differences between natively folded and unfolded states (rms 1.8 ppm) than the other N-terminal amides (rms 4.4 ppm). Assuming that the ^{15}N chemical shifts in the partially folded N-terminal half are similar to those in the natively folded state, the non-vanishing intensities for residues with smaller ^{15}N chemical shift differences suggest that the conformational exchange rate for these residues in the N-terminal folding nucleus[34,35] corresponds to the fast-exchange limit, *i.e.*, occurs on a sub-millisecond time scale.

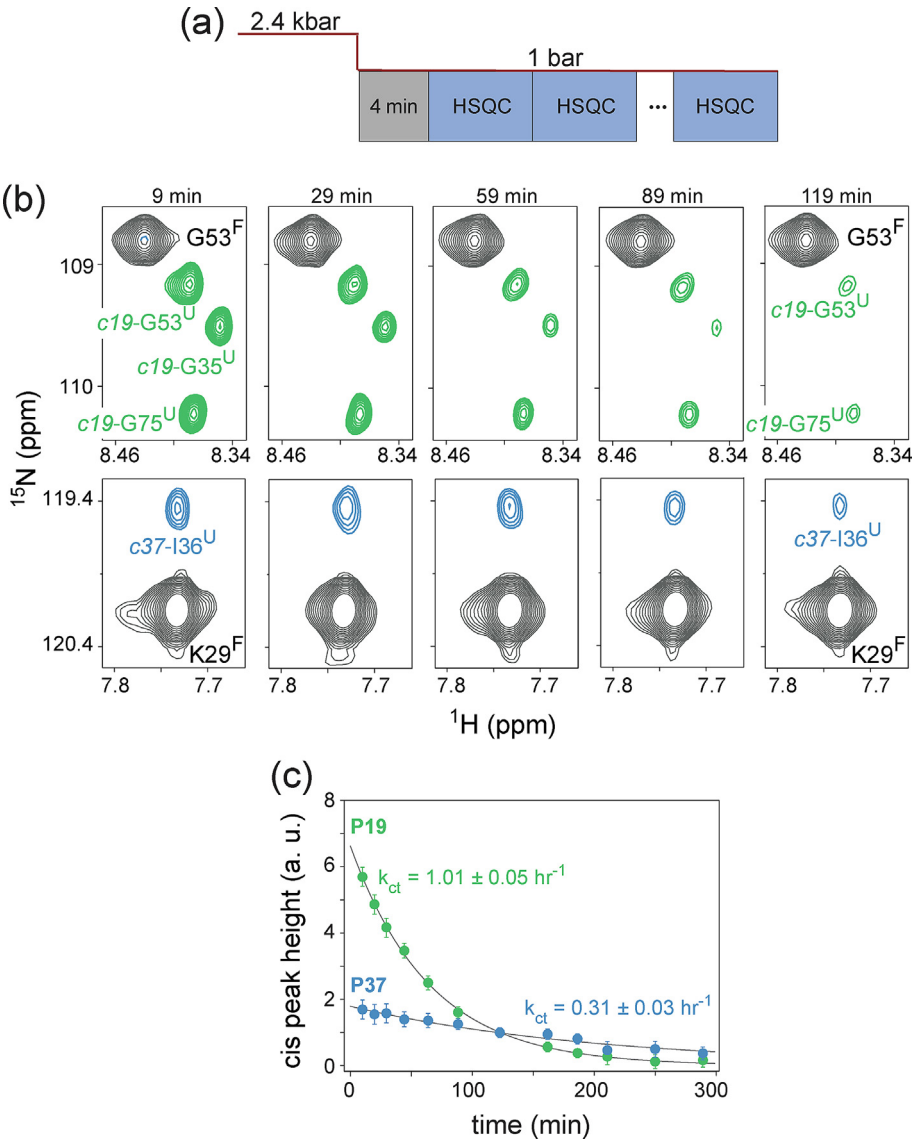

Figure 2. Proline *cis* to *trans* isomerization kinetics under folding conditions at 267.9 K. (a) Schematic timing diagram for single-jump, low-pressure readout HSQC experiments. After 3.5 h of Pro *cis*/*trans* equilibration while in the unfolded state at 2.4 kbar, the pressure is dropped to 1 bar. Following a 4-min delay for temperature equilibration and shimming, a series of HSQC spectra is collected over a total duration of 5 h. (b) Expanded regions of 800-MHz HSQC spectra (10 min each). Spectra track the disappearance of the *cis* isomer with time after the pressure drop for the unfolded state resonances of G53, G35 and G75, corresponding to *cis*-P19 (top row, green), and I36 for *cis*-P37 (bottom row, blue). Indicated time points correspond to the mid-point of each 10-minute measurement. (c) P19 and P37 *cis* to *trans* isomerization rates determined from mono-exponential fits of the corresponding *cis* intensities *vs* time after pressure drop.

Remarkably, and in contrast with *cis*-P19, few resonances at near-random-coil positions are observed for the *cis*-P37 isomer at 267.9 K, namely those of I36 and D39 (Figure S6). Their intensities decay more than five-fold slower after the pressure drop than signals of the *cis*-P19 chains (Figure 2c). This observation suggests that the remaining residues in *cis*-P37 chains are either exchange-broadened and therefore invisible in the NMR spectrum, or that their resonances closely overlap with those of the natively folded protein. In the latter case, *cis* to *trans* isomerization of P37 would not impact the intensity of these native state resonances. Therefore, the two possibilities can be distinguished by monitoring the intensities of the folded state after the pressure drop: In the case of exchange-broadening, intensities of the natively folded state will increase by 5.2% after this *cis*-P37 fraction of chains has reverted to *trans* at

very long times after the pressure drop (assuming 5.2% *cis*-P37 at the time of the pressure drop; see Methods). This increase adds to the intensity increase resulting from the *ca* 7.8% *cis*-P19 chains isomerizing to *trans* at the k_{ct} rate of P19. Measurement of a small intensity change for the folded ubiquitin resonances as a function of time at a precision better than 1% is experimentally challenging because it requires high signal to noise, extreme spectrometer stability, and spectra with perfect baseline properties. Such spectra (Figure S8) were acquired at 900 MHz using the SOFAST-HMQC method,[26] showing that the recovery of folded intensities at 276 K clearly is bi-exponential, with the larger (7.8%) and faster (3.26/hr) recovering fraction assigned to P19, and the slower fraction (5.2%; 0.68/hr) corresponding to P37 (Figure 3b).

The rate of P38 isomerization under folding conditions is too fast for measurement with the above pressure-drop method because G35 and D39 signals for the *cis*-P38 chains are intrinsically low due to the low *cis*-P38 population, and its rapid isomerization to *trans* under folding conditions causes these peaks to fall below the detection threshold already in the first spectrum recorded after the pressure drop (Figure S6, S8).

Isomerization kinetics from double pressure-jumps

For measurement of the rapidly isomerizing P38 under folding conditions, we carried out "double jump" experiments, somewhat analogous to the double-jump, stopped-flow, unfolding-refolding experiments on ribonuclease-A by Houry et al.[36] These double-jump experiments then also provided an independent second measurement for the above reported isomerization rates of P19 and P37, validating the method.

In our double pressure-jump experiments, the protein is first equilibrated under unfolding conditions at high pressure, then the pressure is dropped to 1 bar for variable delay time, T_{LP}, after which the pressure is jumped back to high pressure (Figure 4a). This sequence is followed by a rapid readout of the *cis* fraction in the unfolded state at high pressure using the SOFAST-HMQC scheme 26. For $T_{LP} \ll 1/k_{ct}$, amides of residues adjacent to each of the Pro residues have intensities during readout that correspond to the equilibrium *cis* fraction at high pressure. However, when T_{LP} is increased, the *cis* isomer fraction at the start of the high-pressure 2D readout spectrum scales with $p_{eq}\ \exp(-k_{ct}T_{LP})$, where p_{eq} is the equilibrium *cis* fraction at high pressure and k_{ct} is the *cis* to *trans* isomerization rate under folding conditions at atmospheric pressure. A minor complication in the analysis of such double-jump experiments arises from *trans* → *cis* isomerization that occurs while recording the SOFAST-HMQC spectrum at high pressure: Even if the protein were fully refolded with all-*trans* isomers at the end of T_{LP}, *cis* signals will slowly grow in with each t_1 increment of the SOFAST-HMQC due to isomerization in the pressure-denatured state. Note that the last t_1 increments of each SOFAST-HMQC spectrum are recorded by up to several minutes after the pressure is jumped back to 2.4 kbar. While the net integral of such signals in the 2D HMQC spectrum will be zero because that integral corresponds to the first data point in the t_1 time domain, the peak height of *cis* isomer resonances is impacted by the isomerization that takes place during the high-pressure readout sequence. This contribution will be small if the duration of the SOFAST-HMQC

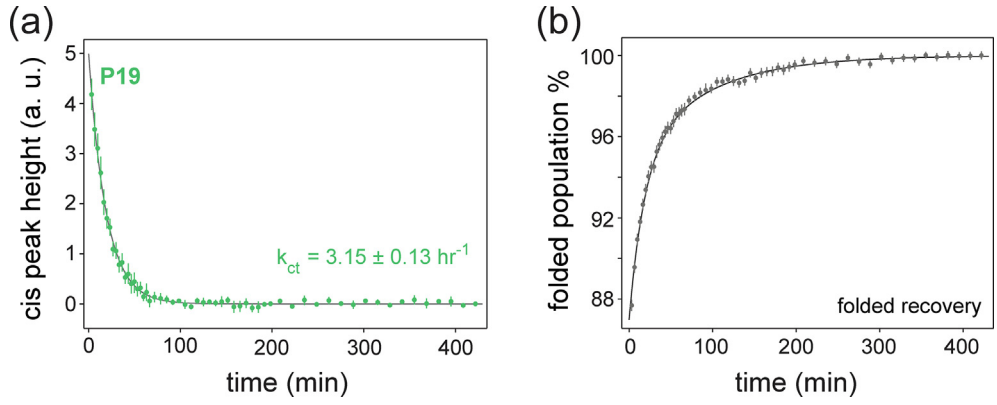

Figure 3. Pro isomerization kinetics at low pressure and 276 K, recorded after a pressure drop from 2.4 kbar to 1 bar. (a) Mono-exponential decay fit of the averaged intensity of 21 well resolved unfolded resonances (Figure S6) from the C-terminal half of ubiquitin that correspond to *cis*-P19. (b) Slow phase of the biexponential intensity recovery observed for resonances of the natively folded spectrum in 900-MHz SOFAST-HMQC spectra (3 mins each), resulting from Pro-19 and Pro-37 isomerization. The solid line corresponds to $I(t) = 87 + 7.8(1\text{-}e^{-t/3.26}) + 5.2(1\text{-}e^{-t/0.68})$ where I(t) is the averaged intensity of folded amide resonances at time *t* (hr) after the pressure drop.

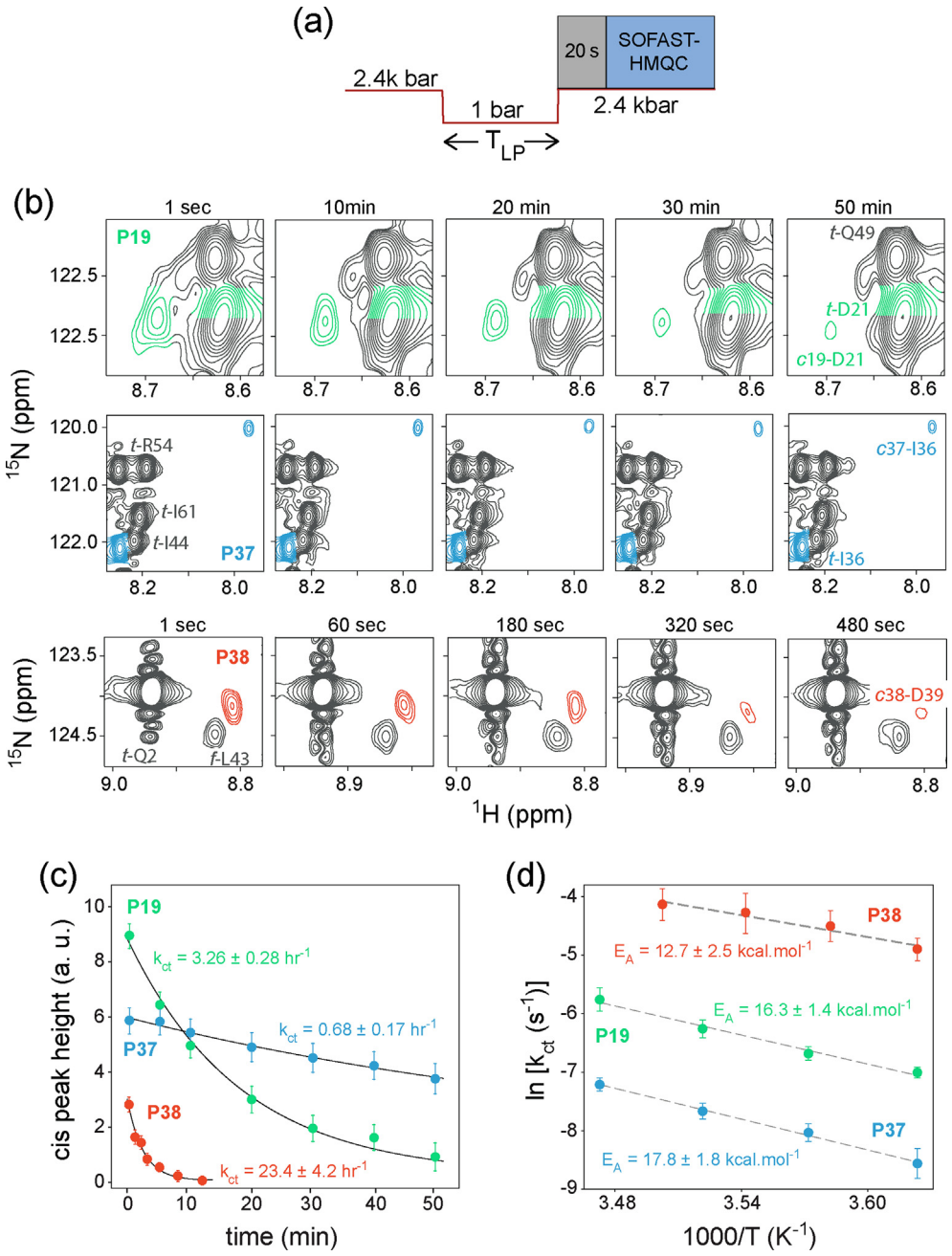

Figure 4. Measurement of proline isomerization by double pressure-jump NMR. (a) Schematic timing diagram for the double-jump, SOFAST-HMQC readout experiment. A single 2D NMR spectrum is collected for each value of the low-pressure delay, T_{LP}. SOFAST-HMQC spectra (1 min each) were recorded at 600 MHz, 276 K, using two scans per FID. The first scan was delayed 20 s to allow time for the temperature to equilibrate. Multiple spectra were recorded for each T_{LP} and co-added prior to analysis to improve S/N. (b) Expanded regions, showing the disappearance of *cis* isomers at low pressure. (top row) D21, corresponding to *cis*-P19; (middle row) I36, for *cis*-P37; (bottom row) D39, for *cis*-P38. The nearby intense unfolded signals for *trans*-P19 (green) and *trans*-P37 (blue), corresponding to the isomer population at the end of T_{LP}, are also shown. The signal marked *f*-L43 represents residual L43 intensity for the small fraction of folded protein at 2.4 kbar. (c) Mono-exponential decay fits for the intensities of D21 (green: *cis*-P19), I36 (blue: *cis*-P37) and D39 (red, *cis*-P38). For other temperatures, see Figure S10. (d) Temperature dependence of k_{ex} for the three Pro residues, and corresponding Arrhenius activation energies, E_A.

experiment is short relative to $1/k_{ex}$, where k_{ex} is the isomerization rate at high pressure (obtained from Figure 1). With these rates known, their effect on the NMR intensities is predicted to give rise to a small, known offset when fitting the *cis* isomer intensities as a function of T_{LP}. The predicted

offset (Supporting Information) is very small at low temperature where the total time for collecting the SOFAST-HMQC spectrum (~1 min.) is very short relative to $1/k_{ex}$, but it becomes noticeable at 288 K where k_{ex} is faster.

The *cis* → *trans* isomerization rates measured with the double-jump experiments for the three Pro residues under folding conditions span a very wide range, with rapid isomerization observed for P38, but a *ca* 50-fold slower rate for P37 (Figure 4), which makes it difficult to optimize the measurement for all three Pro residues simultaneously. The most time-consuming step of the measurement involves establishing *cis*–*trans* equilibria at high pressure, which for P37 requires more than 8 h at 276 K. However, with the steep temperature dependence of the isomerization rate, equilibration can be expedited by performing it, in part, at 298 K (see Methods). For P38, which isomerizes much faster, establishing equilibrium populations is faster, and its measurements can be repeated much more rapidly. Therefore, separate sets of double-jump experiments were carried out for measurement of the slowly isomerizing P19 and P37, and for the more rapidly isomerizing P38. For the latter, the duration of the SOFAST-HMQC measurement was reduced to 1 min by using a very short interscan delay, such as to minimize the effect of P38 isomerization during the high-pressure readout. Four repeats of the entire series of spectra were co-added to improve the signal to noise for these weak *cis*-P38 signals, whereas only two repeats were averaged for P19 and P37.

For both P19 and P37, we found that the k_{ct} rates and their activation energies measured under folding conditions at atmospheric pressure remained relatively close to those observed under denaturing conditions at high pressure (Figure 4c, d). The *ca* twofold lower rates at high pressure in part reflect the effect of pressure on the isomerization rate of Pro residues in unstructured polypeptides,[31] also seen for the two linear heptapeptides analyzed by us which showed a 1.6-fold decrease in isomerization rate at high pressure (SI Figure S5). In contrast to P19 and P37, *cis* → *trans* isomerization of P38 is nearly an order of magnitude faster at atmospheric pressure than under denaturing, high-pressure conditions (Figure 4). The temperature dependence of the P19 and P37 *cis*–*trans* isomerization rates yielded Arrhenius activation energies under folding conditions at 1 bar (Figure 4d) that were only slightly lower than in the pressure-denatured state (Figure 1d). By contrast, a drop from 18.9 ± 1.1 kcal/mole at high pressure to 12.7 ± 2.5 kcal/mole at low pressure for P38 is substantial and appears responsible for the much faster isomerization of this residue under folding conditions.

Discussion

Pressure jump NMR spectroscopy makes it possible to study proteins under non-equilibrium conditions at atomic resolution. A range of applications has been proposed and explored,[17] opening new opportunities to gain atomic level insights into protein folding and oligomerization.[18,19] Our analysis of proline isomerization in both the denatured and native states represents yet another capability enabled by this powerful but technically challenging pressure-jump NMR methodology. In contrast to studies of protein folding, where pressure jumps need to be faster than the folding and unfolding time scales (milliseconds to seconds), Pro isomerization typically occurs on a time scale of minutes. Therefore, even relatively slow changes in pressure, on the time scale of multiple seconds, which are accessible to conventional high-pressure NMR accessories,[37] will suffice to study the isomerization process. However, spectrometer control of such hardware from within the pulse sequence program will be essential for synchronizing the pressure changes with the collection of NMR signals. Our study relied on home-built hardware that switched pressure in *ca* 3 ms (for the interval stretching from 10 to 90% of the desired pressure change), with faster jumps possible by removing flow restrictors that were inserted in the pressure-transducing tubing for applications where high speed was not essential.

Proline isomerization rates measured by us in pressure-denatured ubiquitin, including their activation energies, are consistent with prior measurements in linear peptides and chemically denatured proteins.[1,32,38] A key question, however, concerns the rate of isomerization under folding conditions, *i.e.* at atmospheric pressure, where it is considered the rate-limiting step for protein chains containing non-native Pro isomers.[1,32,39] A *ca* 1.6-fold higher isomerization rate at atmospheric pressure is expected relative to 2.4 kbar based on the activation volume, $\Delta V^{\ddagger} \approx 5.4$ cm^3/mol, measured by us for two heptapeptides. However, an approximate doubling of the isomerization rate is observed for P19 and P37, slightly larger than the compounded experimental uncertainty in the measured rates. By contrast, a much larger, *ca* 8-fold increase in isomerization rate is observed for P38. Such a large increase is only possible if the isomerization barrier height is lowered under conditions where the protein folds, requiring the presence of a partially folded species. Unfortunately, the P38 *cis*-to-*trans* isomerization rate is too high, and therefore the lifetime of such a folding intermediate too short, for recording its 2D ^{1}H-^{15}N spectrum at the high signal to noise needed for observing this <3% *cis*-P38 fraction of protein immediately after the pressure drop.

Evidence for partially folded states of *cis*-P19 and *cis*-P37 isomers emerges from the spectra observed immediately after the pressure drop. For *cis*-P19, sharp unfolded resonances for the C-terminal half of the protein imply a protein state where the N-terminal half is in an exchange-broadened state that must involve a partially folded intermediate (Figure S7). The intense, narrow signal for S20 indicates that this residue remains highly disordered also in this partially folded state, while weak resonances for G10, *K*11, T14, V26, and A28, which have ^{15}N resonance frequencies close to random coil values, imply a sub-millisecond exchange process between this semi-folded state and the fully unfolded state. Such a rapid exchange process was seen previously by pressure-jump NMR for residues Q2-E18 in the V17A/V26A ubiquitin mutant,[18] and is consistent with partial population of a β-hairpin that persists even under denaturing conditions of 8 M urea, pH2.5.[40] For the *cis*-P19 isomer of L50A ubiquitin, the partially folded state also involves residues D21-D32 that comprise the first α-helix in native ubiquitin, where it packs against its β −sheet in what is often considered to be an obligatory early intermediate on ubiquitin's folding pathway.[34,35] It appears that the *cis*-P19 chains can adopt a similar 'folding nucleus'. However, the carbonyl oxygen of *cis*-P19 in this intermediate would be unable to make the two long-range H-bond interactions to S57-H^N and S57-H$^\gamma$ that stabilize ubiquitin in its natively folded state,[41] thereby preventing the folding process from progressing beyond this early intermediate.

For *cis*-P37 isomers, that have lifetimes longer than 1 h at temperatures below 280 K, unfolded state resonances could only be identified for nearby residues I36 and D39 at 267.9 K. Our observation that all native-state, folded HMQC resonances show a 5% component that recovers slowly at the k_{ct} rate of P37 (Figure 3b) indicates that *cis*-P37 isomers adopt an exchange-broadened state that involves essentially the entire protein, which contrasts with what is seen for *cis*-P19 isomers. Considering the absence of sharp, unfolded resonances that disappear at the P37 k_{ct} rate, it appears likely that this exchange-broadened state involves the same residues as the natively folded state. This observation suggests that it is structurally similar to the folded state, but that unfavorable interactions in the loop region comprising *cis*-P37 and P38 prevent it from adopting a well-ordered state, resulting in a molten globule where intermediate time scale dynamics obliterate the NMR signals.[42,43] Similar behavior likely also applies for *cis*-P38 isomers, but due to its much faster isomerization it was not possible to positively identify the absence of the corresponding protein resonances prior to isomerization of P38 to its native *trans* state. However, the considerable increase in isomerization rate and concomitant decrease in activation energy relative to the pressure-denatured state imply a folded structure where strain on the P37-P38 peptide bond lowers its isomerization barrier height.

Our ubiquitin results highlight that the kinetics of the slow steps in protein folding associated with *cis–trans* proline isomerization can differ substantially from those in linear peptides. Whereas the lowering of the peptide bond isomerization activation energy was found to be small (*ca* 13%) for both P19 and P37, a *ca* 33% lower value was observed for P38. Therefore, on a quantitative level, the slowdown in protein folding kinetics caused by requisite proline isomerization can be substantially slower than expected based on peptide-derived isomerization kinetics.

The presence of partially structured states during folding of protein chains containing non-native proline isomers has long been recognized,[44] and their important role in aggregation and amyloid formation underscores the biological relevance of such states.[45] Our data provide positive evidence implicating *cis* forms of both P19 and P37 in formation of partially folded structures that encompass half (P19) or all (P37) of the protein chain. Ubiquitin's third proline (P38) isomerizes too fast under native folding conditions to observe the residues involved it its partially folded structure. However, the lowered activation energy for P38 isomerization strongly implicates the presence of a partially folded species. Our finding that for each of the three Pro residues in this small, single domain protein, the presence of a non-native isomer leads to a partially folded structure implies that formation of such structures may be much more common than generally assumed.

CRediT authorship contribution statement

Elahe Masoumzadeh: Writing – original draft, Investigation, Formal analysis, Conceptualization. **Jinfa Ying:** Writing – review & editing, Investigation. **James L. Baber:** Writing – review & editing, Resources, Methodology. **Philip Anfinrud:** Writing – review & editing, Resources, Methodology. **Ad Bax:** Writing – review & editing, Supervision, Methodology, Conceptualization.

DECLARATION OF COMPETING INTEREST

The authors declare that they have no known competing financial interests or personal

relationships that could have appeared to influence the work reported in this paper.

Acknowledgments

We thank D.A. Torchia and W.A. Eaton for helpful discussions, and Tobin Sosnick for suggesting the study of the L50A mutant. This work was supported by the Intramural Research Program of the National Institute of Diabetes and Digestive and Kidney Diseases.

Appendix A. Supplementary data

Supplementary data to this article can be found online at https://doi.org/10.1016/j.jmb.2024.168587.

Received 1 March 2024;
Accepted 17 April 2024;
Available online 23 April 2024

Keywords:
protein folding;
hydrostatic pressure;
NMR spectroscopy;
peptide bond isomerization;
molten globule

References

1. Wedemeyer, W.J., Welker, E., Scheraga, H.A., (2002). Proline cis-trans isomerization and protein folding. *Biochemistry* **41**, 14637–14644.
2. Eichner, T., Radford, S.E., (2009). A generic mechanism of β_2-microglobulin amyloid assembly at neutral pH involving a specific proline switch. *J. Mol. Biol.* **386**, 1312–1326.
3. Stoller, G., Rücknagel, K.P., Nierhaus, K.H., Schmid, F.X., Fischer, G., Rahfeld, J.U., (1995). A ribosome-associated peptidyl-prolyl cis/trans isomerase identified as the trigger factor. *EMBO J.* **14**, 4939–4948.
4. Kawagoe, S., Nakagawa, H., Kumeta, H., Ishimori, K., Saio, T., (2018). Structural insight into proline cis/trans isomerization of unfolded proteins catalyzed by the trigger factor chaperone. *J. Biol. Chem.* **293**, 15095–15106.
5. Fischer, G., Bright, W.-L., Lang, K., Kiefhaber, T., Schmid, F.X., (1989). Cyclophilin and peptidyl-prolyl cis-trans isomerase are probably identical proteins. *Nature* **337**, 476–478.
6. Theriault, Y., Logan, T.M., Meadows, R., Yu, L., Olejniczak, E.T., Holzman, T.F., Simmer, R.L., Fesik, S.W., (1993). Solution structure of the cyclosporin A/cyclophilin complex by NMR. *Nature.* **361**, 88–91.
7. Bosco, D.A., Eisenmesser, E.Z., Pochapsky, S., Sundquist, W.I., Kern, D., (2002). Catalysis of cis/trans isomerization in native HIV-1 capsid by human cyclophilin A. *Proc. Natl. Acad. Sci. USA* **99**, 5247–5252.
8. Moore, J.M., Peattie, D.A., Fitzgibbon, M.J., Thomson, J. A., (1991). Solution structure of the major binding-protein for the immunosuppressant FK506. *Nature* **351**, 248–250.
9. Pastorino, L., Sun, A., Lu, P.J., Zhou, X.Z., Balastik, M., Finn, G., Wulf, G., Lim, J., et al., (2006). The prolyl isomerase Pin1 regulates amyloid precursor protein processing and amyloid-β production. *Nature* **440**, 528–534.
10. Namanja, A.T., Wang, X.J., Xu, B., Mercedes-Camacho, A. Y., Wilson, K.A., Etzkorn, F.A., Peng, J.W., (2011). Stereospecific gating of functional motions in Pin1. *Proc. Natl. Acad. Sci. USA* **108**, 12289–12294.
11. Alderson, T.R., Lee, J.H., Charlier, C., Ying, J., Bax, A., (2018). Propensity for cis-proline formation in unfolded proteins. *Chembiochem* **19**, 37–42.
12. Mateos, B., Conrad-Billroth, C., Schiavina, M., Beier, A., Kontaxis, G., Konrat, R., Felli, I.C., Pierattelli, R., (2020). The ambivalent role of proline residues in an intrinsically disordered protein: from disorder promoters to compaction facilitators. *J. Mol. Biol.* **432**, 3093–3111.
13. Grathwohl, C., Wuthrich, K., (1976). The X-Pro peptide bond as an NMR probe for conformational studies of flexible linear peptides. *Biopolymers* **15**, 2025–2041.
14. Mallis, R.J., Brazin, K.N., Fulton, D.B., Andreotti, A.H., (2002). Structural characterization of a proline-driven conformational switch within the Itk SH2 domain. *Nature Struct. Biol.* **9**, 900–905.
15. Lu, K.P., Finn, G., Lee, T.H., Nicholson, L.K., (2007). Prolyl cis-trans isomerization as a molecular timer. *Nature Chem. Biol.* **3**, 619–629.
16. Schmidpeter, P.A.M., Schmid, F.X., (2015). Prolyl Isomerization and its catalysis in protein folding and protein function. *J. Mol. Biol.* **427**, 1609–1631.
17. Kremer, W., Arnold, M., Munte, C.E., Hartl, R., Erlach, M. B., Koehler, J., Meier, A., Kalbitzer, H.R., (2011). Pulsed pressure perturbations, an extra dimension in NMR spectroscopy of proteins. *J. Am. Chem. Soc.* **133**, 13646–13651.
18. Charlier, C., Alderson, T.R., Courtney, J.M., Ying, J., Anfinrud, P., Bax, A., (2018). Study of protein folding under native conditions by rapidly switching the hydrostatic pressure inside an NMR sample cell. *Proc. Natl. Acad. Sci. USA* **115**, 201803642.
19. Chiliveri, S.C., Shen, Y., Baber, J.L., Ying, J.F., Sagar, V., Wistow, G., Anfinrud, P., Bax, A., (2023). Experimental NOE, chemical shift, and proline isomerization data provide detailed insights into amelotin oligomerization. *J. Am. Chem. Soc.* **145**, 18063–18074.
20. Herberhold, H., Winter, R., (2002). Temperature- and pressure-induced unfolding and refolding of ubiquitin: a static and kinetic Fourier transform infrared spectroscopy study. *Biochemistry* **41**, 2396–2401.
21. Roche, J., Caro, J.A., Norberto, D.R., Barthe, P., Roumestand, C., Schlessman, J.L., Garcia, A.E., Garcia-Moreno, E.B., et al., (2012). Cavities determine the pressure unfolding of proteins. *Proc. Natl. Acad. Sci. USA* **109**, 6945–6950.
22. Roche, J., Dellarole, M., Caro, J.A., Guca, E., Norberto, D. R., Yang, Y.S., Garcia, A.E., Roumestand, C., et al., (2012). Remodeling of the folding free energy landscape of staphylococcal nuclease by cavity-creating mutations. *Biochemistry* **51**, 9535–9546.

23. Ying, J., Delaglio, F., Torchia, D.A., Bax, A., (2017). Sparse multidimensional iterative lineshape-enhanced (SMILE) reconstruction of both non-uniformly sampled and conventional NMR data. *J. Biomol. NMR.* **68**, 101–118.
24. Delaglio, F., Grzesiek, S., Vuister, G.W., Zhu, G., Pfeifer, J., Bax, A., (1995). NMRpipe – a multidimensional spectral processing system based on Unix pipes. *J. Biomol. NMR.* **6**, 277–293.
25. Skinner, S.P., Fogh, R.H., Boucher, W., Ragan, T.J., Mureddu, L.G., Vuister, G.W., (2016). CcpNmr AnalysisAssign: a flexible platform for integrated NMR analysis. *J. Biomol. NMR.* **66**, 111–124.
26. Schanda, P., Kupce, E., Brutscher, B., (2005). SOFAST-HMQC experiments for recording two-dimensional heteronuclear correlation spectra of proteins within a few seconds. *J. Biomol. NMR.* **33**, 199–211.
27. Maltsev, A.S., Grishaev, A., Roche, J., Zasloff, M., Bax, A., (2014). Improved cross validation of a static ubiquitin structure derived from high precision residual dipolar couplings measured in a drug-based liquid crystalline phase. *J. Am. Chem. Soc.* **136**, 3752–3755.
28. Alderson, T.R., Lee, J.H., Charlier, C., Ying, J.F., Bax, A., (2018). Propensity for cis-proline formation in unfolded proteins. *Chembiochem* **19**, 37–42.
29. Brandts, J.F., Halvorson, H.R., Brennan, M., (1975). Consideration of possibility that slow step in protein denaturation reactions is due to cis-trans isomerism of proline residues. *Biochemistry.* **14**, 4953–4963.
30. Schmid, F.X., Baldwin, R.L., (1978). Acid catalysis of formation of slow-folding species of Rnase-A – evidence that reaction is proline isomerization. *Proc. Natl. Acad. Sci. USA* **75**, 4764–4768.
31. Hauer, H., Ludemann, H.D., Jaenicke, R., (1982). Free activation energies and activation volumes for the amide rotation in some peptides studied by high-pressure 1H high resolution NMR. *Z. Naturforschung C-a J. Biosci.* **37**, 51–56.
32. Reimer, U., Scherer, G., Drewello, M., Kruber, S., Schutkowski, M., Fischer, G., (1998). Side-chain effects on peptidyl-prolyl cis/trans isomerisation. *J. Mol. Biol.* **279**, 449–460.
33. Jeener, J., Meier, B.H., Bachmann, P., Ernst, R.R., (1979). Investigation of exchange processes by two-dimensional NMR spectroscopy. *J. Chem. Phys.* **71**, 4546–4553.
34. Sosnick, T.R., Dothager, R.S., Krantz, B.A., (2004). Differences in the folding transition state of ubiquitin indicated by phi and psi analyses. *Proc. Natl. Acad. Sci. USA* **101**, 17377–17382.
35. Piana, S., Lindorff-Larsen, K., Shaw, D.E., (2013). Atomic-level description of ubiquitin folding. *Proc. Natl. Acad. Sci. USA* **110**, 5915–5920.
36. Houry, W.A., Rothwarf, D.M., Scheraga, H.A., (1994). A very fast phase in the refolding of disulfide-intact ribonuclease A – implications for the refolding and unfolding pathways. *Biochemistry* **33**, 2516–2530.
37. Peterson, R.W., Wand, A.J., (2005). Self-contained high-pressure cell, apparatus, and procedure for the preparation of encapsulated proteins dissolved in low viscosity fluids for nuclear magnetic resonance spectroscopy. *Rev. Sci Instrum.*, 76.
38. Grathwohl, C., Wuthrich, K., (1981). NMR studies of the rates of proline cis-trans isomerization in oligopeptides. *Biopolymers* **20**, 2623–2633.
39. Jackson, S.E., Fersht, A.R., (1991). Folding of chymotrypsin inhibitor-2. Influence of proline isomerization on the folding kinetics and thermodynamic characterization of the transition state of folding. *Biochemistry.* **30**, 10436–10443.
40. Meier, S., Strohmeier, M., Blackledge, M., Grzesiek, S., (2007). Direct observation of dipolar couplings and hydrogen bonds across a beta-hairpin in 8 M urea. *J. Am. Chem. Soc.* **129**, 754–755.
41. Vijay-Kumar, S., Bugg, C.E., Cook, W.J., (1987). Structure of ubiquitin refined at 1.8 A resolution. *J. Mol. Biol.* **194**, 531–544.
42. Christensen, H., Pain, R.H., (1991). Molten globule intermediates and protein folding. *Eur. Biophys. J.* **19**, 221–229.
43. Dyson, H.J., Wright, P.E., (2004). Unfolded proteins and protein folding studied by NMR. *Chem. Rev. (Washington, DC, United States)* **104**, 3607–3622.
44. Reader, J.S., Van Nuland, N.A.J., Thompson, G.S., Ferguson, S.J., Dobson, C.M., Radford, S.E., (2001). A partially folded intermediate species of the β-sheet protein apo-pseudoazurin is trapped during proline-limited folding. *Protein Sci.* **10**, 1216–1224.
45. Jahn, T.R., Parker, M.J., Homans, S.W., Radford, S.E., (2006). Amyloid formation under physiological conditions proceeds via a native-like folding intermediate. *Nature Struct. Mol. Biol.* **13**, 195–201.